ARMA 17-559

Investigating the Role of Temperature on Thermal Stress and Fracture Propagation in Geothermal Systems

Mohsen Bazargan, Pooyan Broumand, Agust Gudmundsson
Royal Holloway University of London, Egham, United Kingdom
Philip Meredith, Mohsen Bazargan,
University College London, London, United Kingdom
Ali Rezaee, Soliman Mohammed
Houston university, Houston, United States of America

ABSTRACT: Available geothermal energy extractable by conventional techniques is in dry and comparatively impermeable rocks. Enhanced Geothermal System (EGS) technologies enhance geothermal resources in the hot dry rock (HDR) through fracture operations, usually through hydro-shearing. Large scale deployment of geothermal power production requires the demonstration of successful EGS projects extracting heat from reservoirs constituting a variety of geological conditions. In this part, numerical models are very important to show how geothermal power plant operations can be less risky and safer. Owing the fact that, some major challenges in these operations are interaction between shear and tensile fractures with natural faults. These interactions can be seen in two different cases, either these faults are badly oriented or these faults are fill in pore fluids or gases which are mainly high pressure. Fluids and gases are important on account for because of the fact that these pore fluids can over whelmed the injection pressure and cause well blow out. Furthermore, to prevent these operational hazards, we use field data and analysis in combination with experimental tests and numerical/analytical models with finite element method software such as COMSOL Multiphysics. Further work will be required for improving enhanced geothermal production by optimizing hydro-shearing practices.

1. INTRODUCTION

Geothermal energy resources have been used by mankind in some form for thousands of years. Depending on the temperature of the resource, it may be used for power production, supply of heat or a combination of both. In order to expand the potential for geothermal power production, focus should be made on facilitating the deployment of the Enhanced Geothermal System (EGS) technology. In this work, we investigate the role of temperature of injecting or pore fluids and gases for thermal stressing in rock texture and check these influences on numerical models.

To predict the fracture propagation system in geothermal reservoirs, numerical models should be able to show the temperature effects. This effect can cause small thermal expansions and generate thermal stresses. Also, thermal stress experiments have shown that cooling contraction produces a greater abundance of fractures in comparison with thermal expansion. Within an overall tensile cooling regime Mode, I crack propagate in small increments to make generally longer fractures. Finally, in our models we show how we can predict this temperature dependent fracture propagation system which is an additional propagation parameter in the system. Hydraulic fracturing (HF) is one of the best techniques employed in oil and gas reservoirs to improve the turnover of production. In this phenomenon a highly pressurized fluid is pumped into a borehole resulting in creation of cracks which will be used to reach in stored resources in hard layers reported by Dong e.g. Primary models of HF have assumed a neat crack evolving in a continuous medium which has been proved to be over idealized as nearly all reservoirs are full of faults affecting this phenomenon. The existence of faults – especially very large ones – could far change the crack propagation mechanisms; different behaviors of penetration, arrest, diversion and offset could be distinguished in case intersection takes place by Zhang e.g. Multiple parameters will be important in final behavior of the intersecting cracks; fluid viscosity, angle between interfaces, crack lengths,

friction coefficient and far field stresses. But these parameters were not considered in these set of presenting models. HF in medias with initial faults has been studied by different methods. Akulich and Zvyagain have studied interaction between HF crack and natural fractures using a BEM procedure, where viscosity effects have been taken into account. Simulation of hydraulic fracture propagation near a natural fracture using virtual multidimensional internal bonds is represented by Zhang and Ghassemi. Zhang et al. has studied layered medium where the effects of different sequences of soft and stiff layers has been investigated. Gudmunsson and Brenner have performed similar study with more than two layers taken into account.
In this paper the finite element method will be used to model HF in sedimentary rock samples and its interaction with natural faults. The crack tip behavior will be assumed to be linear, where asymptotic enrichment functions will be employed.
The contact between surfaces of the natural fault is modeled. The HF is assumed to be non-viscous, producing a uniform pressure over the interface where no leak-off is considered for the current along the crack into the domain. Stress intensity factor based criteria are employed for the fracture initiation and propagation direction detection.
Finally, in order to show the accuracy and robustness of the proposed algorithms several numerical examples are presented. HF is a handful process employed extensively in different engineering applications. One of the most appealing uses is in oil industry where HF is applied in order to break hard layers of rocks to reach pressurized oil and gas reservoirs. In such cases, massive amount of fluids – especially water – is injected into reservoirs resulting in breakage of hard layers.
This method is very common and significantly improves the total revenue of the field. The simulations were performed by Comsol multiphysics.

2. GOVERNING EQUATIONS

Consider a body Ω as shown in Fig1. With boundary Γ that consists of external parts of Γ_t and Γ_u referred to loaded and restrained zones together with internal discontinuities of Γ_d which could be both pressurized or traction free. The Lagrangian framework is employed in order to implement the formulation, thus the reference configuration is used. And the continuity equation results in $\rho J = \rho_0$, where J is the determinant of deformation gradient.
Assuming quasi-static condition, the equilibrium equation could be written as follows,

$$\nabla.\boldsymbol{\sigma} + \rho\mathbf{b} = 0 \qquad (1)$$

Where $\mathbf{b}$ is the body force per unit mass vector which is generally gravity, ρ is the average density of the medium and $\boldsymbol{\sigma}$ is the Cauchy stress tensor.

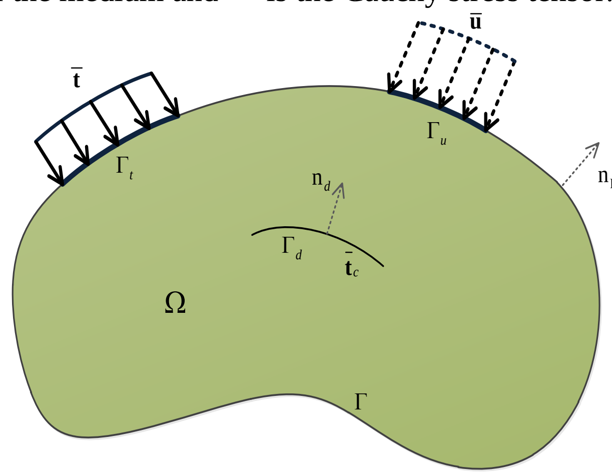

Figure 1. Free body diagram in state of equilibrium. The boundary conditions could be summarized as below.

$$\boldsymbol{\sigma}.\mathbf{n}_\Gamma = \bar{\mathbf{t}} \quad \text{on } \Gamma_t \qquad (2a)$$

$$\mathbf{u} = \bar{\mathbf{u}} \quad \text{on } \Gamma_u \qquad (2b)$$

$$\boldsymbol{\sigma}.\mathbf{n}_d = \bar{\mathbf{t}}_c \quad \text{on } \Gamma_d \qquad (2c)$$

Where $\mathbf{n}_\Gamma$ and $\mathbf{n}_d$ are the unit normal vector to the internal or external boundaries respectively.
The constitutive equation relating the stress to the total strain is expressed by means of an incrementally linear stress-strain relationship as follows,

$$\mathrm{d}\boldsymbol{\sigma} = \mathbf{D}\mathrm{d}\boldsymbol{\varepsilon} \qquad (3)$$

Where, in the above relation $\mathbf{D}$ is the tangential elastic tensor of the continuum. In this section weak form of expression (1) will be derived, where the trial function for the displacement field, $\mathbf{u}(\mathbf{X},t)$, is assumed satisfying all essential and natural boundary conditions while being smooth enough to define derivatives of equations. Moreover, the test function $\delta\mathbf{u}(\mathbf{X},t)$ is also required to have the properties of trial function. The classic procedure of the finite element is employed in order to derive the weak form of the equilibrium equation, where $\delta\mathbf{u}(\mathbf{X},t)$ is multiplied by equation (1) and is integrated over the domain in initial configuration. It follows,

$$\int_{\Omega}\delta\mathbf{u}.(\nabla.\boldsymbol{\sigma}+\rho\mathbf{b})\,d\Omega=0 \qquad (4)$$

Next, the discontinuous divergence theorem is employed find the weak form.. As the domain includes internal discontinuities, this theorem results in extra terms over these boundaries [see 11]. It follows,

$$\int_{\Omega}(\nabla\delta\mathbf{u})^{T}:\boldsymbol{\sigma}\,d\Omega+\int_{\Gamma_d}\delta\mathbf{u}.\boldsymbol{\sigma}\mathrm{n}_d\;\;d\Gamma=\int_{\Omega}\delta\mathbf{u}.\rho\mathbf{b}\,d\Omega+\int_{\Gamma}\delta\mathbf{u}.\bar{\mathbf{t}}\,d\Gamma, \qquad (5)$$

Where the term $\int_{\Gamma_d}\delta\mathbf{u}.\boldsymbol{\sigma}\mathrm{n}_d\;\;d\Gamma$ accounts for the tractions applied to the internal interface, which is zero for traction free conditions. In this investigation, for the sake of simplicity, the effects of fluid viscosity are ignored since it is negligible for water as the propelling fluid. This assumption results in a constant pressure distribution over the interface. Considering equation (5), the term $\mathbf{t}=\boldsymbol{\sigma}.\mathbf{n}$ on upper and lower crack faces is equal to fluid pressure on crack faces i.e. $\boldsymbol{\sigma}\mathbf{n}_d=-p\mathbf{n}_d$. Hence,

$$\int_{\Gamma_d}\delta\mathbf{u}.\boldsymbol{\sigma}\mathrm{n}_d\;\;d\Gamma=\int_{\Gamma_d}\delta\mathbf{u}.p\mathrm{n}_d\;\;d\Gamma \qquad (6)$$

The crack propagation criterion is

$$F=K_I-K_{Ic}=0 \qquad (7)$$

where, $K_I=\sqrt{\pi a_k}(\sigma_n+p+f(a_k)s_n)$ (8)

The consistency equation implies that $\dot{F}=0$

$$\frac{\dot{a}_k\sqrt{\pi}}{2\sqrt{a_k}}(\sigma_n+p+f(a_k)s_n)+\sqrt{\pi a_k}\left(\dot{\sigma_n}+\dot{p}+\frac{df}{da}\dot{a}\,s_n+f(a_k)\dot{s_n}\right)=0 \qquad (9)$$

thus,

$$\dot{a}_k=-\frac{2a_k(\dot{\sigma_n}+\dot{p}+f(a_k)\dot{s_n})}{\sigma_n+p+f(a_k)s_n+2a_k\frac{df}{da}\,s_n} \qquad (10)$$

Under transient condition, without material properties changing or in-situ hear generation, equation (8) can show reliable output [27]:

$$\frac{1}{\alpha}\frac{\partial T}{\partial t}=\frac{\partial^2 T}{\partial x^2}+\frac{\partial^2 T}{\partial y^2} \qquad (11)$$

Owing the fact that temperature will change by time and in specimen body during heat transfer, then above equation should be discrete by place and temperature. Considering the finite difference formulation, the time can be expressed as:

$$t=p\Delta t \qquad (12)$$

Here Δt is time period.

Using an Euler forward scheme, the temporal discretization of the temperature derivative takes the form Finite difference equation for temperature is like equation (10), in this equation results can be more reliable when Δt decrease.

$$\frac{\Delta T}{\Delta t}_{m,n}\approx\frac{T^{p+1}_{m,n}-T^{p}_{m,n}}{\Delta t} \qquad (13)$$

By placing equation (10) in equation (8) and by assuming $\Delta x=\Delta y$ (that can let us use rectangular meshes) then temperature distribution in p+1 can be detect from equation (11):

$$T^{p+1}_{m,n}=\frac{\alpha\Delta t}{(\Delta x)^2}(T^{p}_{m+1,n}+T^{p}_{m-1,n}+T^{p+1}_{m,n+1}+T^{p}_{m,n-1})+(1-4\frac{\alpha\Delta t}{(\Delta x)^2})T^{p}_{m,n} \qquad (14)$$

To use those above equation to solve currents problems, one Δx from mesh size and one Δt will be considered in the beginning of modeling. During numerical modeling, with decreasing these two parameters and pick smaller numbers make the computational process longer and generate more convergences results. The convergence condition is from equation (12):

$$\frac{\alpha\Delta t}{(\Delta x)^2}\leq\frac{1}{4} \qquad (15)$$

Numerical simulation results

In this section five numerical examples are presented to investigate the validity of the proposed method. The aim of model is to show how these 3 cracks can interact with each other in static situation. The cracks are not propagation and the only aim is to see their interactions. Material properties for all five examples have been given in Table1.

Table 1:Properties of rock

10.2e9	Young Modulus
0.25	Poisson’s Ratio
2700	Solid Density kg/m3
1000	Fluid Density kg/m3
0.21	Porosity %
0.2	Permeability mD

The first example is a plate with three center cracks of the size 0.5m. The plate is subjected to a surface traction of 〖q=10〗^6 Pa in y direction. Figure 2 shows the geometry, boundary conditions and mesh of the first example.

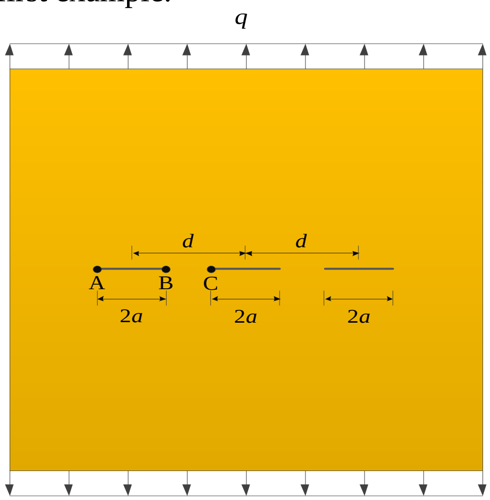

(a)

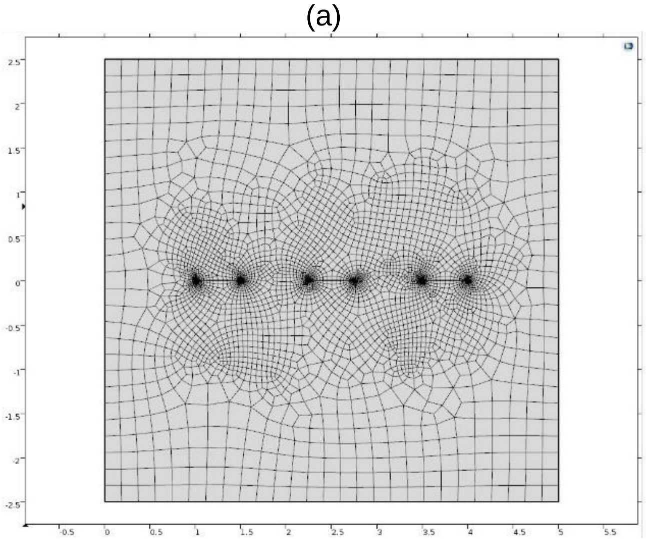

(b)

Figure 2. Three cracks with offset under uniform tension - problem’s configuration.

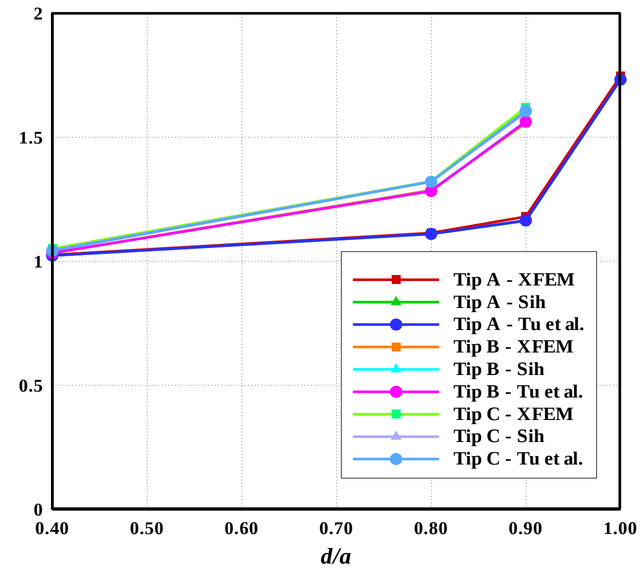

Figure 3. Stress Intensity Factor for plate with three cracks at tips A, B and C.

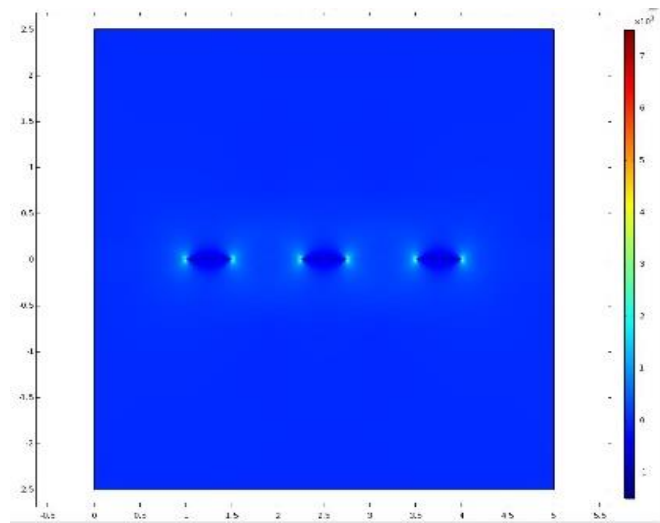

(a)

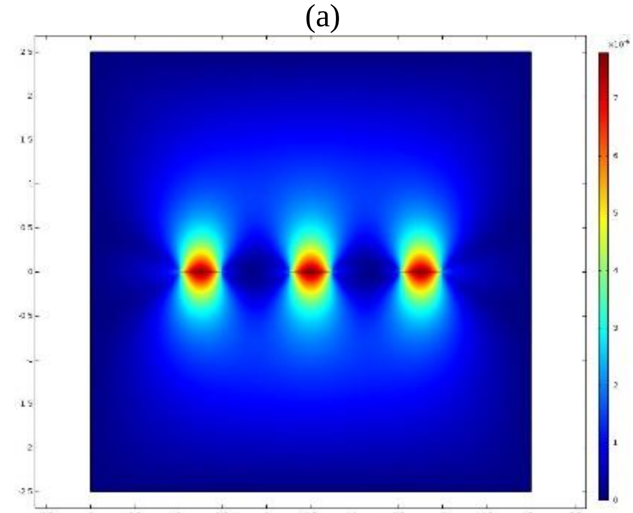

(b)

Figure4. three crack propagation in fixed medium (a) 3rd principal stress (MPa) (b) Displacement of the Y axis (m)

First example will study three cracks with varying distances under uniform tension. Second example will be a single crack with uniform internal pressure which a basic solution for HF where SIFs will be verified with available solutions. Last three problems will study the interaction phenomenon between HF and natural fault. Third example is chosen to show HF crack is propagating in naturally fractured porous medium. This example will study mixed mode crack propagation.

Fourth example is HF crack interacting with natural fault of existing fracture with different directions. This example will study mode I and mixed mode crack propagation. Final simulation is chosen so show what is going to happen after the interaction between HF crack and natural fault in the case of 90 degree angle existing fault in porous medium.

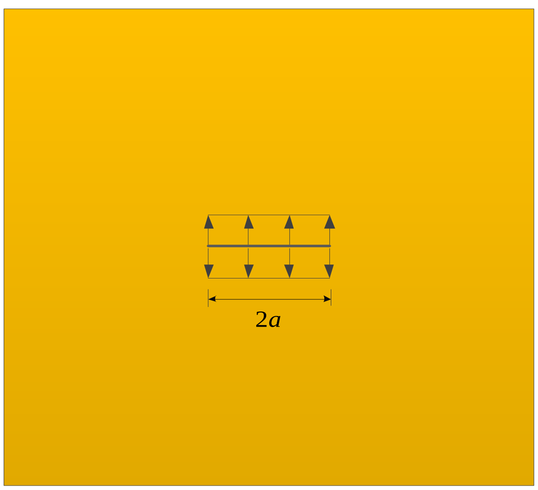

(a)

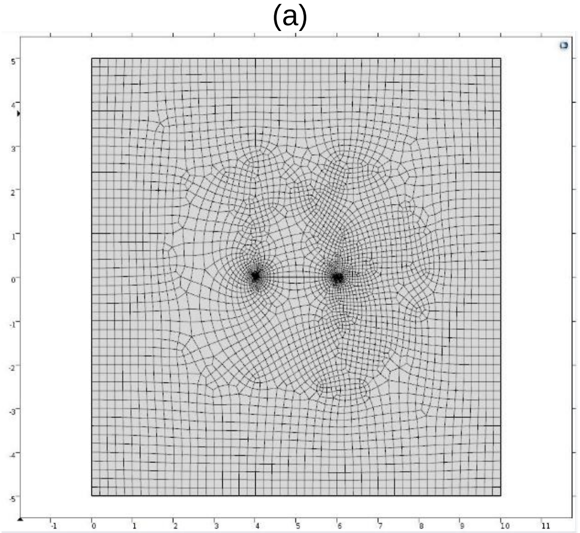

(b)

Figure 5. Single crack subjected to internal pressure – problem's configuration

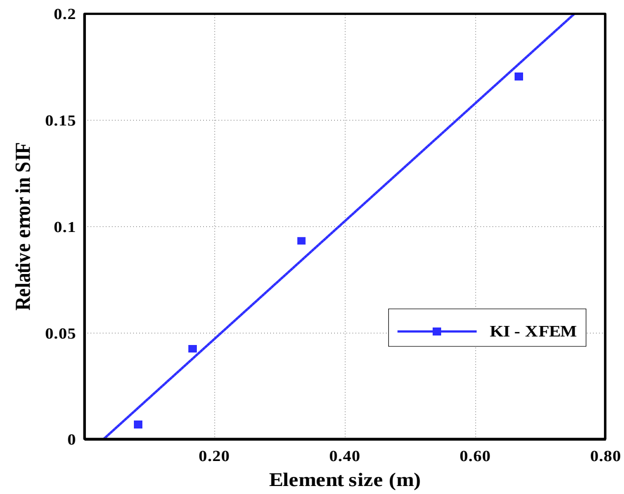

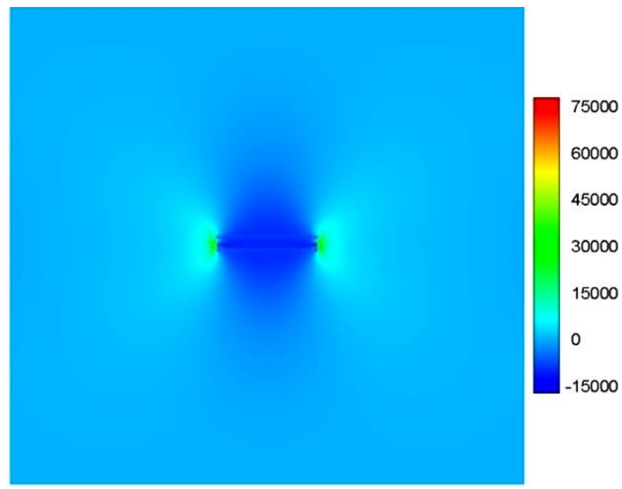

Figure 6. Principal stress and total displacement contours which shown stress concentration around the crack tip and how fracture will propagate.

In the second example the same plate is considered with a single center crack of the size $2a = 2m$. The aim of this model is to show how one crack in intact zone can propagate by pressure inside crack volume. plate of problem 1 is considered with the same material properties. Plain strain condition is assumed. A crack of length 2 meters is positioned at the center of the plate and The crack surface is subjected to a uniform internal pressure of 1e10^6 Pa.

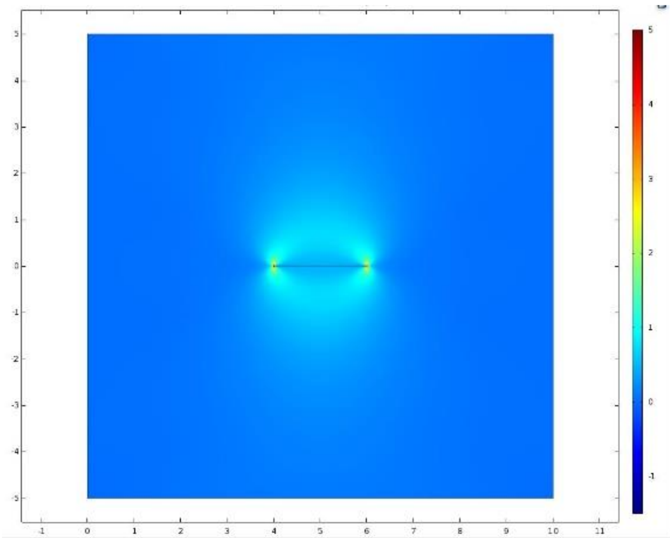

(a)

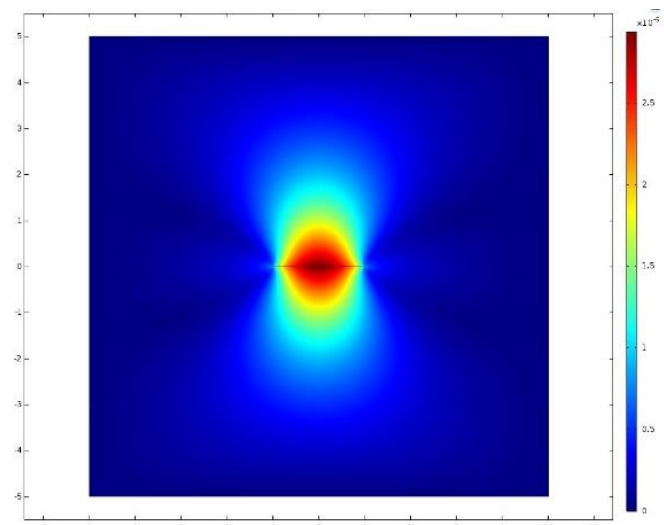

(b)

Figure 7. Single crack propagation in fixed medium (a) 3rd principle stress (GPa) (b) Displacement of the Y axis (cm)

These figures are explaining the hydraulic fracturing propagation of single crack in intact porous medium. Fluid pressure load is the crack wings and the fluid pressure is the only driving force of crack opening and crack growth. Figure 8 shows the natural HF in Bristol channel UK. This field result shows how cracks are propagating between different layers with different material properties. Also, how a single crack can interact with different discontinuities like such as layering and natural fractures and faults.

Figure 8. Field work results on limestone and shale layering. Natural hydraulic fracturing in discontinued and inhomogeneous medium.

In this part of the work we are trying to present the well-known field data when the hydraulic fractures are interacting with natural fault or major natural fracture skeleton. In fact, this example is a preliminary one for modeling HF where next examples will study this loading condition together with propagation in Medias possessing faults. This example with same material properties, HF crack propagating and gets close to 0.5-meter natural fault. In this sample we can observe how HF pressure can effect on natural fault. This set of models are natural faults with three major directions; 30, 90 and150 degree from the propagating fracture.

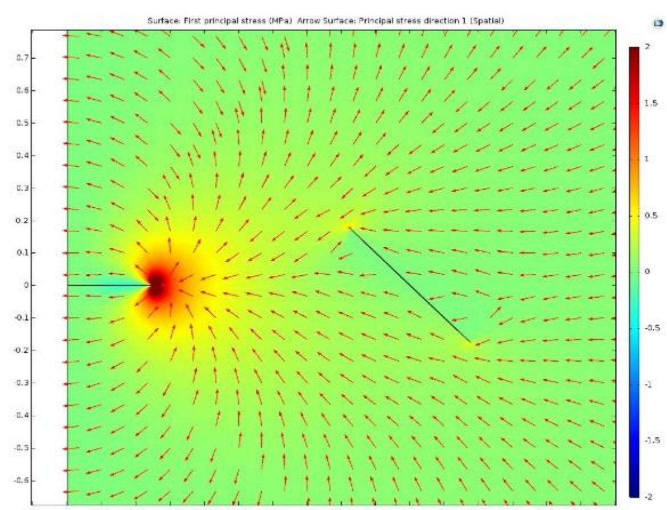

(a)

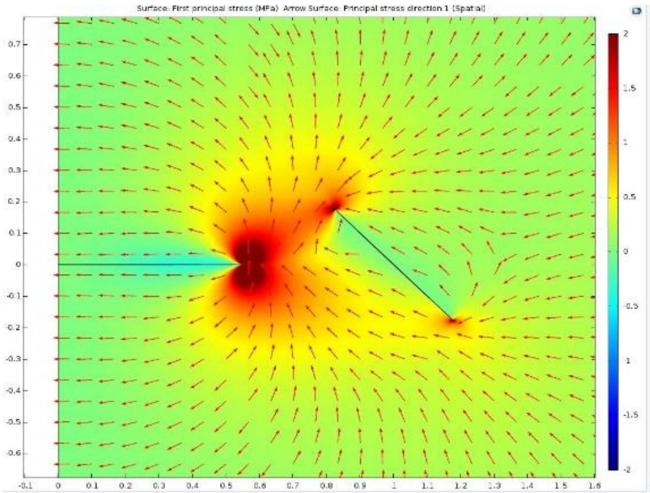

(b)

Figure 9. HF crack in interacting with natural fault and its inside fluid pressure in interacting with edge of 30 degree directed natural fault. (a) 3rd principal stress (GPa) on 100 sec (b) 3rd principal stress (GPa) on 360 sec

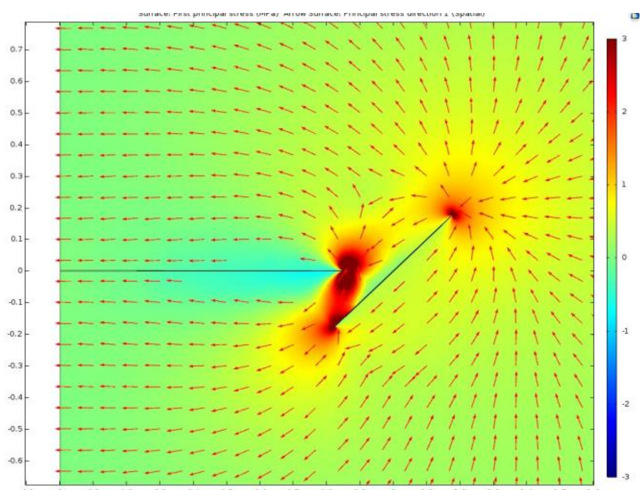

Figure 10. HF crack interaction with 150 degree directed natural fault while the natural fault does have different angels.

Figure 9 and 10 shows how interaction and crack propagation path can change when the HF crack is getting closer to the natural fault. Next example is showing how HF crack interact and propagate in the case with angels' fault is in front of it. Consider the cases of 45-degree angle and 90-degree angle faults and it shows in which case crack propagate on Mode1 and in which crack propagate in mix mode. Despite in primary models for HF simply single crack were assumed and propagated through the medium, empirical cases observed to be very complicated as a variety of parameters play part in this phenomenon. One of the most determinant factors in the probability of existence of natural faults in the media, ending in interaction between these cracks and the driven one. In this simulation we observe how edge of natural fault and final crack path can be both affected by HF crack inside fluid pressure.

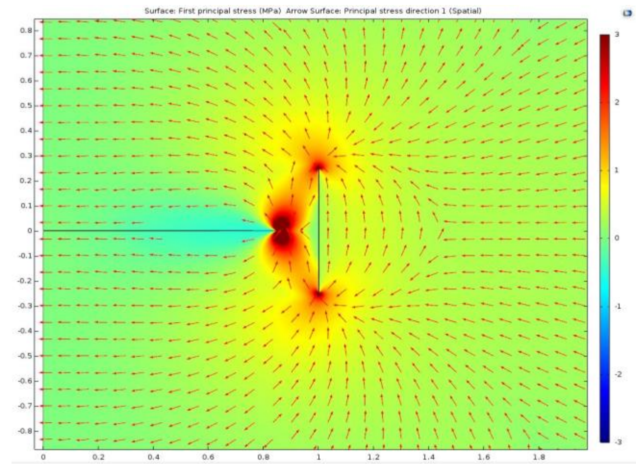

(a)

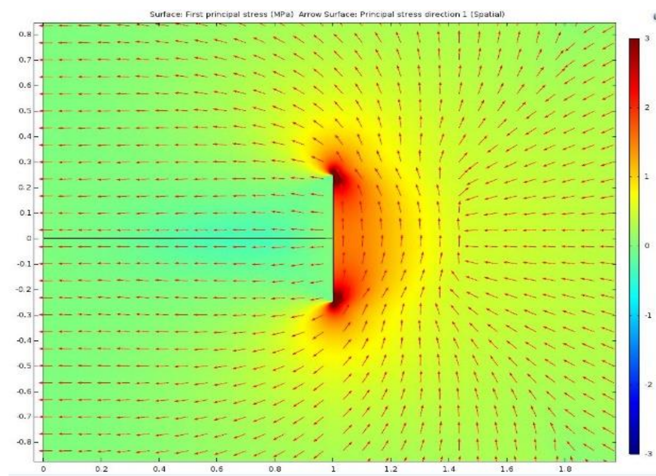

(b)

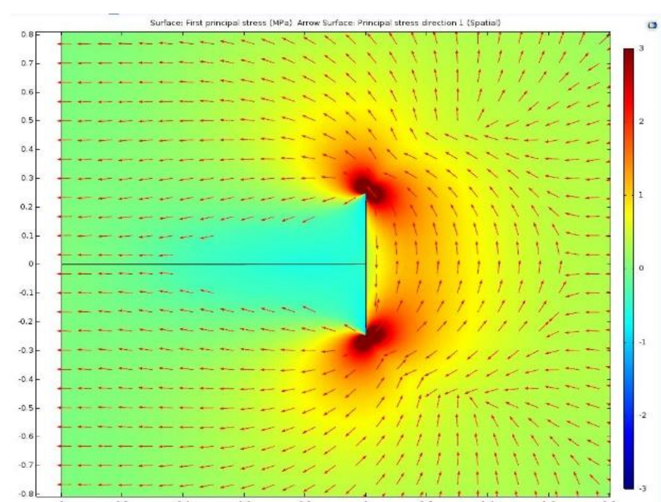

(c)

Figure 11. HF crack in interacting with natural fault and its inside fluid pressure in interacting with edge of 90 degree directed natural fault. (a) 3rd principal stress

(GPa) on 300 sec (b) 3rd principal stress (GPa) on 340 sec (c) 3rd principal stress (GPa) on 390 sec

Fig10 shows in different views what is going to happen after HF crack bond with natural fault and how it is going to effect the propagation afterwards. In different view of the naturally fracture reservoir we can obverse how stress tensor arrows will form to show the area of fault propagation. The main reason of this example is to show how HF crack can continue propagating through natural faults or existing fracture and this process will affect the whole operation.

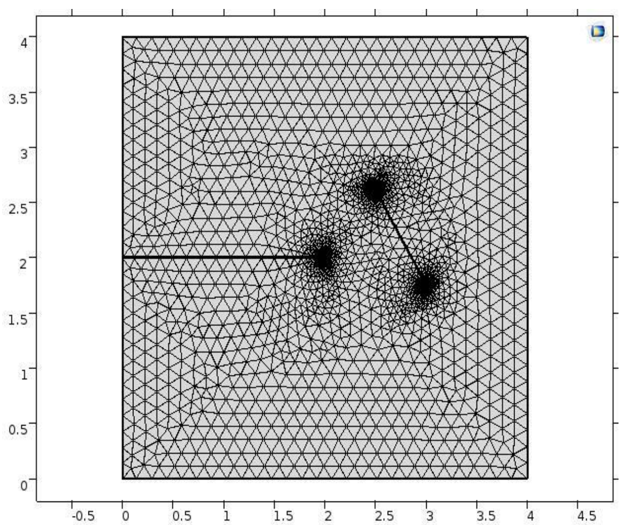

(a)

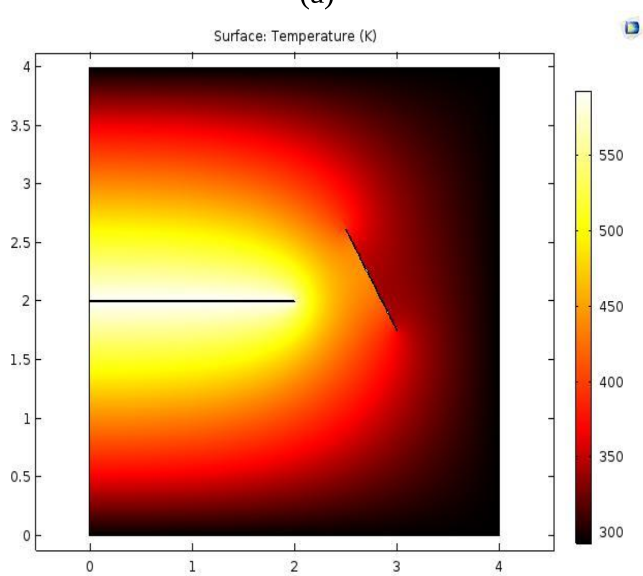

(b)

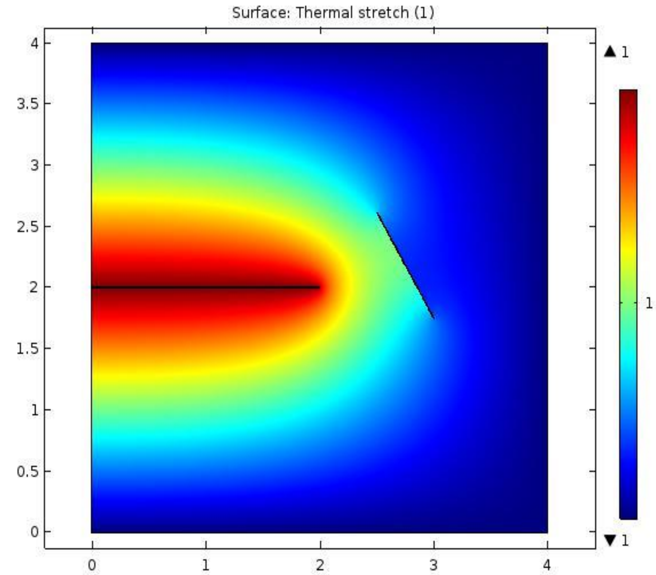

(c)

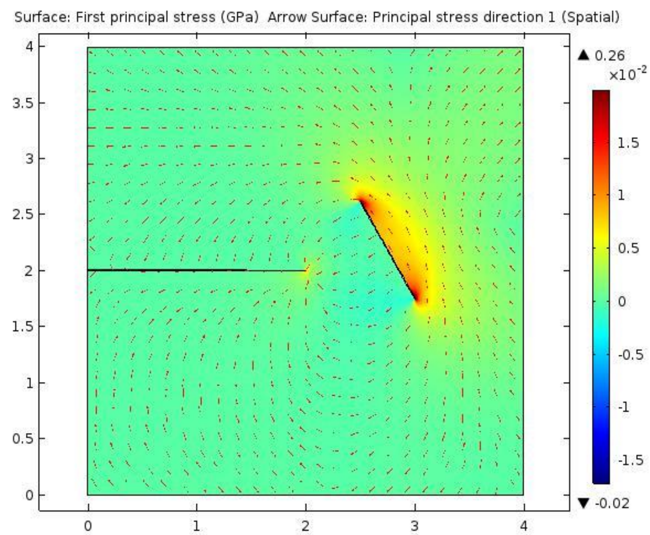

(d)

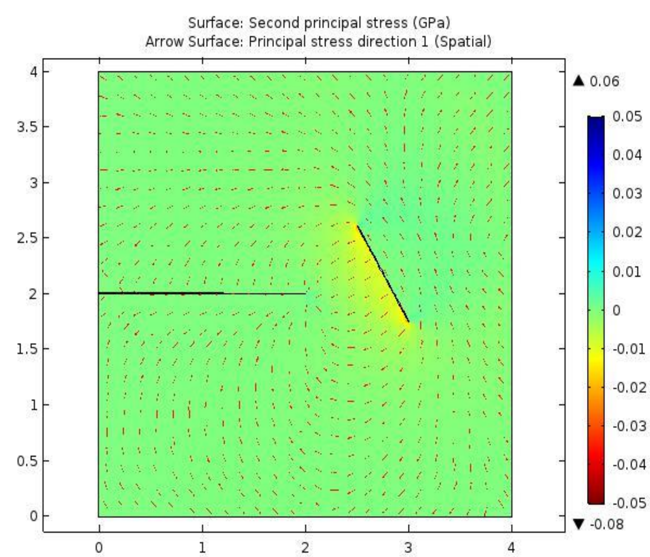

(e)

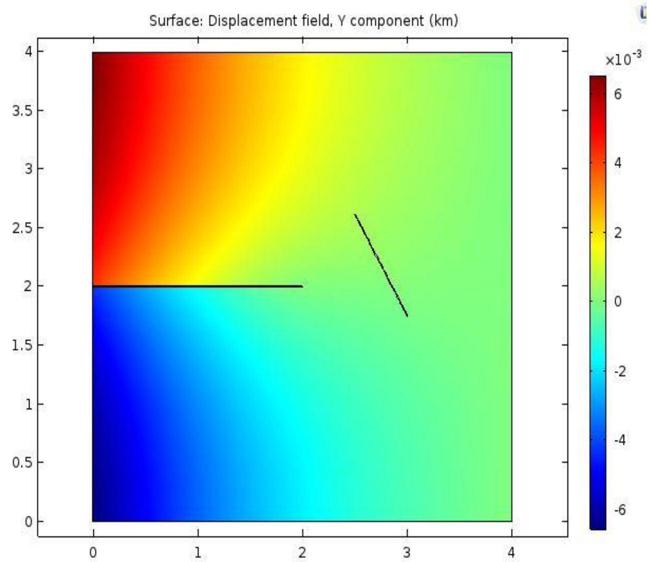

(f)

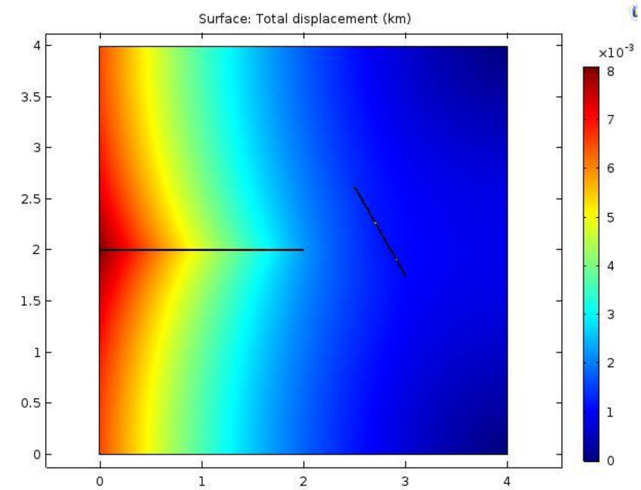

(g)

Figure 12. thermal driving force for initial crack interaction with 30 degree directed natural fault towards the initial fracture a) mesh b) temperature (K) c) thermal stretch (no unit 0-1) d) 1st principal thermal stress (GPa) e) 3rd principal thermal stress (GPa) f) displacement on y axis (cm) g) displacement on x axis (cm)

Fluid temperature on crack propagation alone and show what would happen in fracture propagation when the only force of porous medium breaking is the inside fracture fluid temperature. In this section three models will present thermal fracturing using the parameters from Table-1. In this section initial crack are filled with hot fluid and the temperature is the only driving force in these models. The body temperature in 300K and the temperature inside of the fracture is 600K. In this models natural faults have three major directions of; 30, 90 and 150. In all of these three models it is shown that the thermal stress alone is not going to be effective enough to drive the fracture going further in the medium.

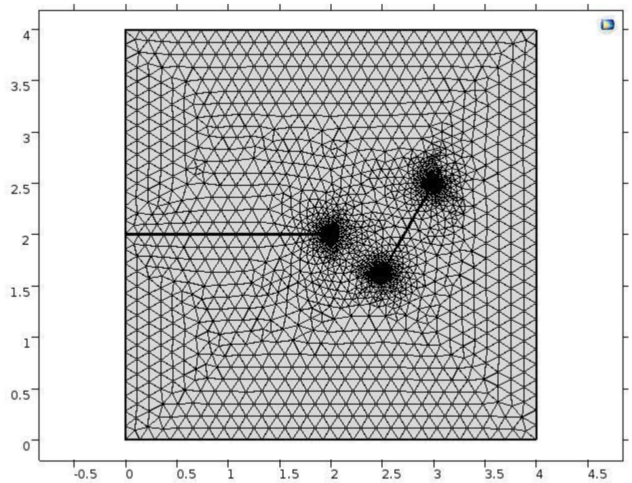

(a)

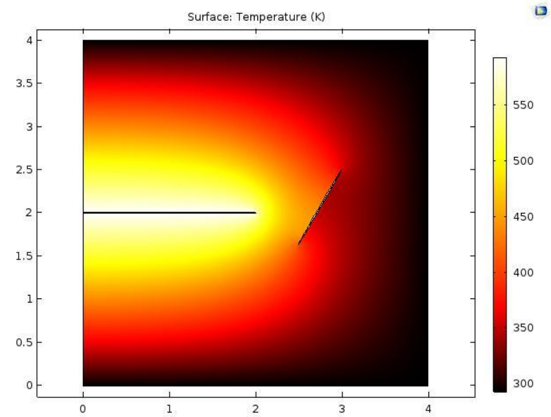

(b)

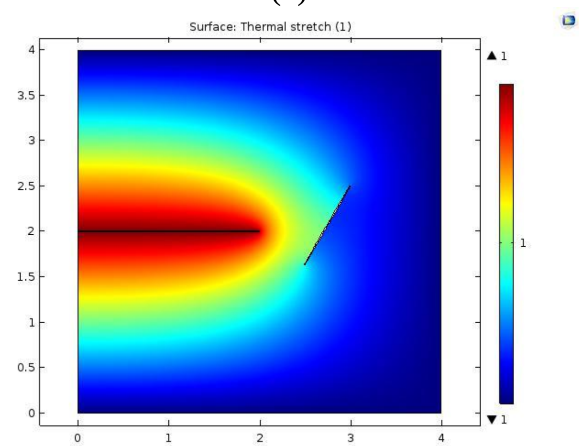

(c)

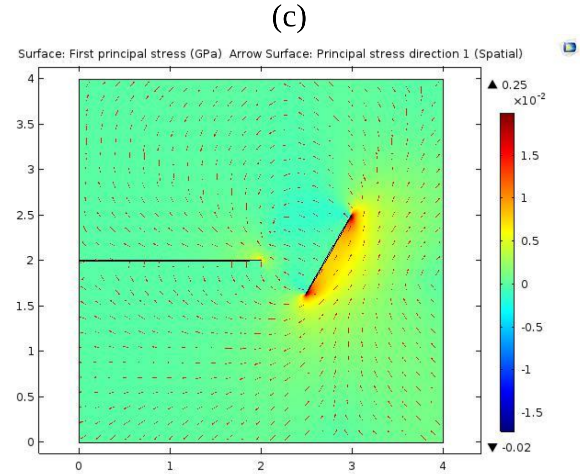

(d)

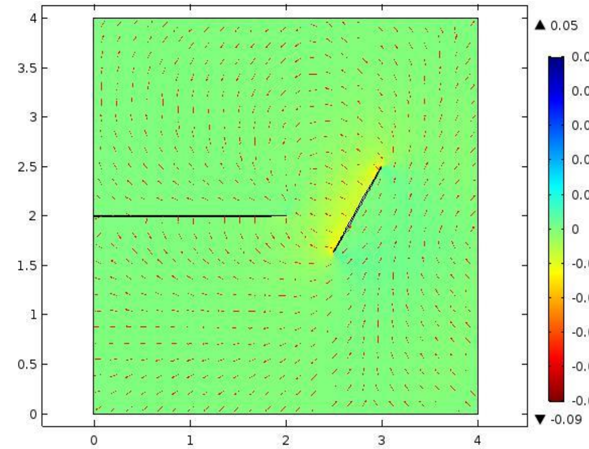

(e)

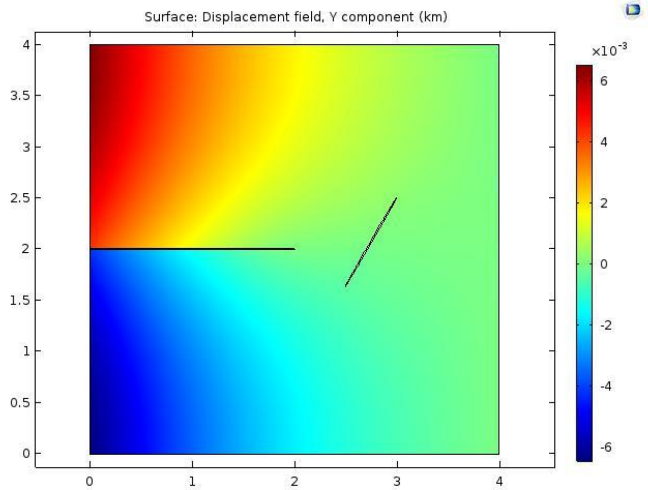

(f)

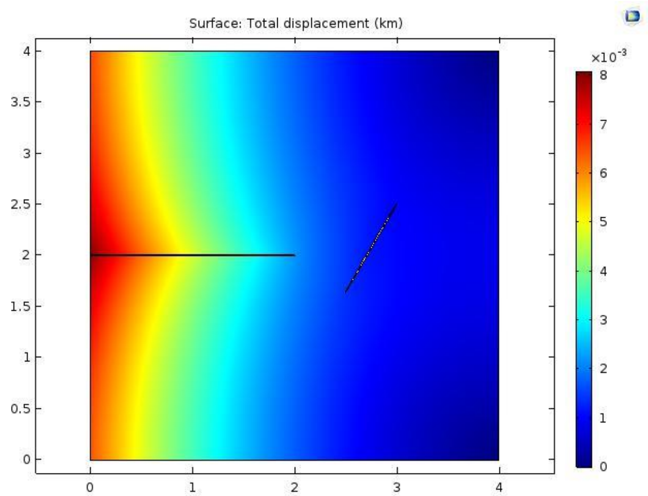

(g)

figure 13. thermal driving force for initial crack interaction with 150 degree directed natural fault towards the initial fracture a) mesh b) temperature (K) c) thermal stretch (no unit 0-1) d) 1st principal thermal stress (GPa) e) 3rd principal thermal stress (GPa) f) displacement on y axis (cm) g) displacement on x axis (cm)

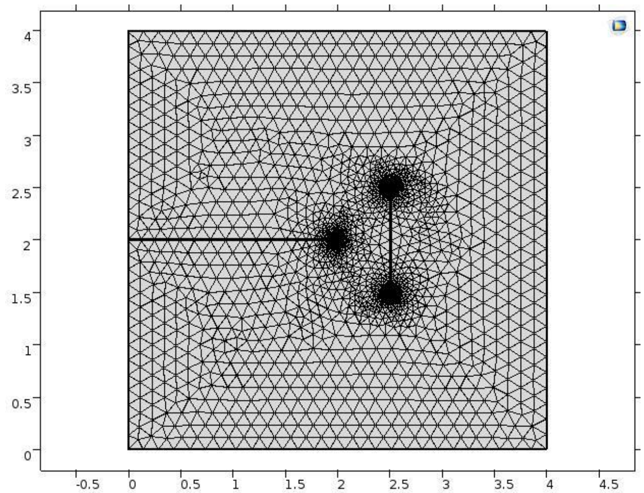

(a)

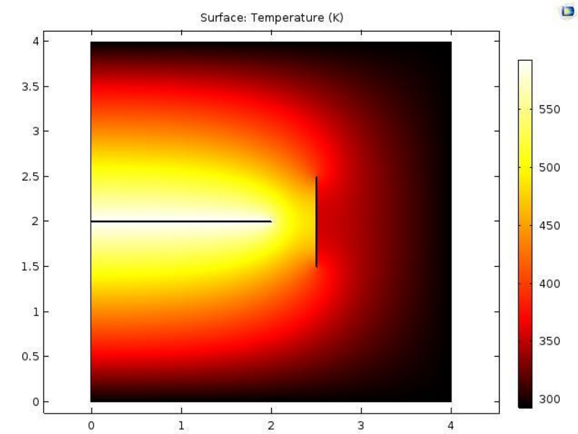

(b)

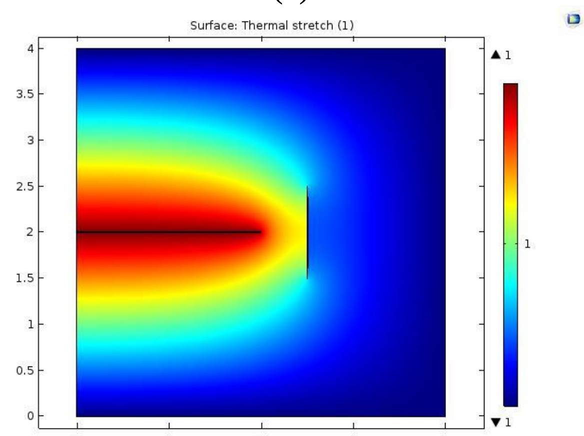

©

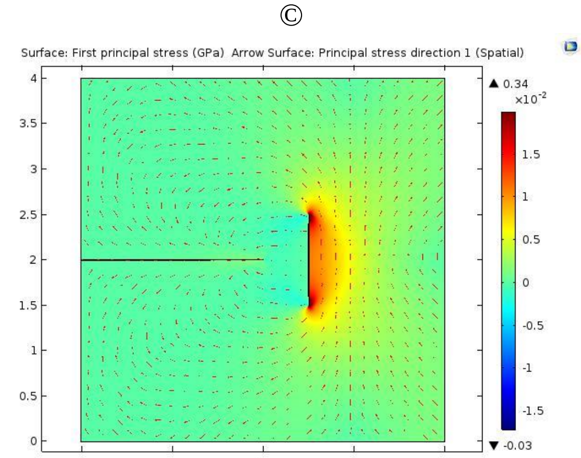

(d)

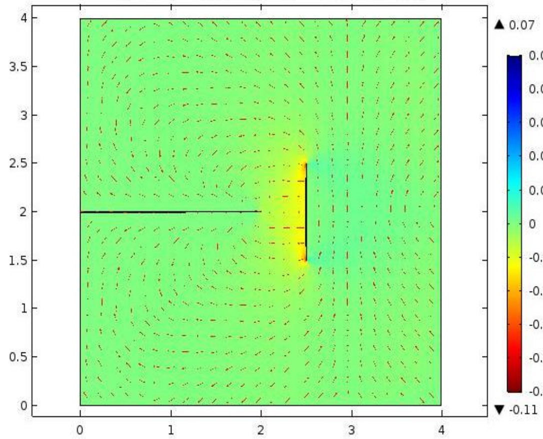

(e)

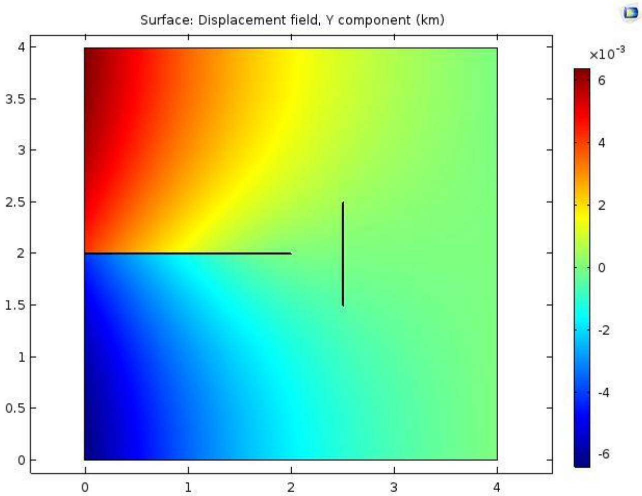

(f)

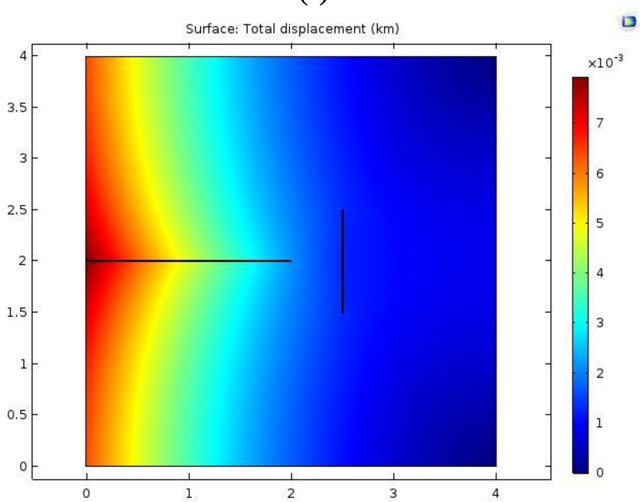

(g)

figure 14. thermal driving force for initial crack interaction with 90 degree directed natural fault towards the initial fracture a) mesh b) temperature (K) c) thermal stretch (no unit 0-1) d) 1st principal thermal stress (GPa) e) 3rd principal thermal stress (GPa) f) displacement on y axis (cm) g) displacement on x axis (cm)

Figure 12, 13 and 14 showing that thermal stresses and temperature effect on fracturing. Their effect will come and coupled with hydraulic fracturing as hot water fracturing. However, these effects are not investigating in this paper.

3. CONCLUSION

In the present paper, the hydraulic fracture propagation was presented in saturated porous media using the finite element method. We observe how it is going to propagate in intact medium or in naturally fractured medium as well. The main reason of risk and hazard control of this paper is all about HF cracks interactions with natural fault and ends up fault propagation. The temperature of the fluid inside fracture just checked as well to show if the stresses that hot fluid can induced in the medium. These fault propagations can easily be flowing the HF fluid to the different area. Some of these badly oriented faults can ends up taking HF fluid to the underground water resources. This is highly unlikely but probable and we investigated it in this report.

ACKNOWLEDGEMENTS

The Author is sincerely thanking IGA for their research grant support. And also Weld on Sweden company and Sharif University of Technology for their contribution.

REFERENCES

1. Akulich AV, Zvyagin AV (2008) Interaction between hydraulic and natural fractures. Fluid Dyn 43: 428–435.
2. Barani OR, Khoei AR, Mofid M (2011) Modeling of cohesive crack growth in partially saturated porous media; A study on the permeability of cohesive fracture. Int J Fracture 167: 15-31.
3. J.N. Germanovich, A.V. Dyskin A model of brittle failure for material with cracks in uniaxial loading Mechanics of Solids, 23 (2) (1988), pp. 111–123.
4. L.N. Germanovich, A.V. Dyskin Fracture mechanisms and instability of openings in compression
5. Int. J. Rock Mech. Min. Sci., 37 (1–2) (2000), pp. 263–284.

6. Dong CY, de Pater CJ (2001) Numerical implementation of displacement discontinuity method and its application in hydraulic fracturing. comput Methods appl Mech Engrg 191: 745-760
7. Lewis RW, Rahman NA (1999) Finite element modeling of multiphase immiscible flow in deforming porous media for subsurface systems. Comput Geotech 24: 41–63.
8. Lewis RW, Schrefler BA (1998) The Finite Element Method in the Static and Dynamic Deformation and Consolidation of Porous Media. Wiley, New York.
9. Zhang Z, Ghassemi A (2011) Simulation of hydraulic fracture propagation near a natural fracture using virtual multidimensional internal bonds. Int J Numer Anal Meth Geomech 35: 480–495.
10. 'Experimental and numerical 2D analysis of hydraulic fracturing using high-power electric discharge', Mohsen Bazargan, Philip Meredith, Nathaniel Forbes Inskip Agust Gudmundsson, Mahdi Habibpour and Reza Mohammadi, June 28 – July 1, 2015, 49th US Rock Mechanics / Geomechanics Symposium held in San Francisco, CA, USA,
11. 'Wellbore instability during plasma torch drilling in geothermal reservoirs', Mohsen Bazargan, Philip Meredith, Nathaniel Forbes Inskip Agust Gudmundsson, M. Soliman, M. Habibpour, A. Rezaei, J. Browning, June 28 – July 1, 2015, 49th US Rock Mechanics / Geomechanics Symposium held in San Francisco, CA, USA,
12. 'Developing Geothermal Energy from Both Hydrothermal and EGS Sources with Considering On Decreasing Risks', Mohsen Bazargan, Philip Meredith, Nathaniel Forbes Inskip Agust Gudmundsson, March 13th, 2015, University of Cambridge, UK. Sedgwick conference
13. 'Hydraulic fracturing in oil and gas resources and its risks and hazards while its interacting with natural faults', Mohsen Bazargan · Agust Gudmundsson · Philip Meredith · Reza Mohammadi, PETEX Conference· Nov 2016
14. Developing Geothermal Energy from Hydrothermal and EGS Sources while Minimizing Risks and hazards', Mohsen Bazargan · Agust Gudmundsson · Philip Meredith · Isaac Kenyon, European Geothermal Congress, Sep 2016